HYDRODYNAMICS CHARACTERIZATION IN PLUNGE POOLS. SIMULATION WITH CFD METHODOLOGY AND VALIDATION WITH EXPERIMENTAL MEASUREMENTS

Luis G. Castillo[1], José M. Carrillo[1]

[1]Department of Civil Engineering, Universidad Politécnica de Cartagena, Spain
Paso Alfonso XIII, 52, 30203 Cartagena, Spain
E-mail: luis.castillo@upct.es, jose.carrillo@upct.es

Abstract

The energy dissipation in plunge pools are produced principally by turbulence generation. In fall jets and in dissipation basins appear high turbulence and aeration phenomena, that cannot be correctly studied by the classical methodologies.

The Hydraulics Laboratory of the Universidad Politécnica de Cartagena (Spain) has an infrastructure designed specifically for the study of turbulent jets and energy dissipation in plunge pools. To improve the knowledge of the phenomenon of turbulent jets, we are measuring aeration rates by means of fiber optical equipment, velocities in different sections of the stilling basin with Doppler instrumentations and pressures on the bottom of the plunge pool with piezoresistive transducers.

The methodology of Computational Fluid Dynamics (*CFD*) simulates the interaction between different fluids, such as the air-water two-phase flows.

The methods used in *CFD* are based on numerical solution of the Reynolds Averaged Navier-Stokes (*RANS*) equations, together with turbulence models of different degrees of complexity. The turbulence models can be classified as either eddy viscosity models (e.g. *k-ε, RNG k-ε, k-ω*) or Reynolds Stress Models (*RSM*). Two equations turbulence models are using to analyze most of the variables involved in the phenomenon, while second-order closure models are employing to obtain a better characterization of the turbulence of the jet.

This paper compares the Parametric theory proposed by Castillo (2006, 2007) for the evaluation of hydrodynamic action in plunge pools, revised by Castillo and Carrillo (2011), with more and new laboratory measurements and the simulation results obtained with *CFD* software *ANSYS CFX* and *FLOW 3D*.

Introduction

The rectangular jet or nappe flow constitutes one of the types of plunge pools in arch dams. The selection of the plunge pool depth is usually a technical and economic decision between a deep pool which needn't lining, or a shallow pool which needs a lining. Therefore, a designer needs to know the magnitude, frequency and extent of the dynamic pressure on the pool floor as a function of the jet characteristics.

The characterization of pressures in plunge pools has been obtained using different scale models: Moore (1943), Lencastre (1961), Ervine and Falvey (1987), Withers (1991), Ervine et al. (1997), Bollaert (2002), Bollaert and Schleiss (2003), Manso et al. (2005) and Federspiel (2011).

In Spain these line of research has been undertaken at Universidad Politécnica de Cataluña by Castillo (1989, 1998), Armengou (1991), Puertas (1994), Castillo et al. (1991, 1999) and at Universidad Politécnica de Cartagena by Castillo (2002, 2006, 2007, 2009, 2010, 2011).

The principal mechanism of energy dissipation are the spreading of the plunging jet (aeration and atomization in the air), air entrainment by the entering jet and diffusion in the pool and finally, the impact with the pool base. For design considerations we define both the issuance conditions and the impingement conditions.

The issuance conditions, located at the exit of the spillway structure, are defined by the mean velocity $V_i = (2gh_0)^{1/2}$, where h_0 is approximately equal twice times the energy head, h.

The principal impingement conditions situated at entrance to the pool are the mean velocity, V_j, and the impingement jet thickness, $B_j = B_g + \xi$, in where B_g is the thickness by gravity conditions and ξ is the jet lateral spread distance by turbulence effect and is approximately equal to the square root of the fall distance (Davies, 1972), and on the other hand, the jet thickness decreases due to gravity effect.

Another important parameter is the jet break-up length, L_b, beyond this distance the jet is completely developed, it no longer contains a core but consists essentially of blobs of water that disintegrate into finer and finer drops. For flows smaller than 0.25 m^2/s (laboratory tests values), the Horeni´s formulae $L_b \sim 6q^{0.32}$ (cited by Ervine et al., 1997) seems to be correct (Castillo, 2006).

For the nappe flow case, Castillo (2006, 2007) proposed some estimators of the turbulence intensity at issuance conditions (T_u^*), jet break-up length (L_b), lateral spread

distance (ξ), impingement thickness (B_j) and the mean dynamic pressure coefficient (C_p).

The turbulence intensity at issuance conditions for laboratory specific flow ($q < 0.25$ m^2/s) is:

$$T_u^* = q^{0.43}/IC \tag{1}$$

IC are the initial conditions with dimensions $[L^{0.86}T^{-0.43}]$:

$$IC = 14.95g^{0.50}/(K^{1.22}C_d^{0.19}) \tag{2}$$

where g is the gravity acceleration, K is a non-dimensional fit coefficient (≈0.85) and C_d the discharge coefficient $[L^{0.5}T^{-1}]$.

The jet break-up length is obtained with the expression:

$$\frac{L_b}{B_i F_i^2} = \frac{K}{\left(K_\varphi T_u F_i^2\right)^{0.82}} \tag{3}$$

being F_i and $T_u = \overline{V_i'}/V_i$ the Froude Number and the turbulent intensity in issuance conditions. $\overline{V_i'}$ and V_i are the *RMS* and mean velocities of the stream wise. $K_\varphi = \overline{V_i'}/w'$ is the turbulence parameter coefficient.

The impingement jet thickness is obtained with:

$$B_j = B_g + 2\xi = \frac{q}{\sqrt{2gH}} + 4\varphi\sqrt{h_0}\left[\sqrt{H} - \sqrt{h_0}\right] \tag{4}$$

where H is the height between upstream water level and downstream water, $\varphi = K_\varphi\, Tu$ is the turbulence parameter in nappe flow case and $h_0 \approx 2h$ the issuance conditions level.

For the mean dynamic pressure coefficient, Castillo (2006) considers two cases:

If $Y \leq 4B_j$:

$$C_p = 0.36(H/L_b)^{-1.04} \tag{5}$$

If $Y > 4B_j$:

$$C_p = \frac{H_m - Y}{V_j^2/2g} = ae^{-b(Y/B_j)} \tag{6}$$

where H_m is the head mean registered at plunge pool bottom (stagnation point), Y is the depth at plunge pool and V_j is the impingement velocity. The parameters a and b of the equation (6) can be obtained from the Table 1.

Table 1: Parameters of the mean dynamic pressure coefficient when $Y > 4B_j$:

H/L_b	a	b	Cp $(Y/B_j > 4)$
< 0.5	0.98	0.070	0.78
0.5-0.6	0.92	0.079	0.69
0.6-0.8	0.65	0.067	0.50
1.0-1.3	0.65	0.174	0.32
1.5-1.9	0.55	0.225	0.22
2.0-2.3	0.50	0.250	0.18
> 2.3	0.50	0.400	0.10

The trajectory of the central nappe is obtained with the Scimeni formulae (1930).

$$x^* = 2.155(y^* + 1)^{\frac{1}{2.33}} - 1$$
$$x^* = x/h; \quad y^* = y/h \tag{7}$$

where x and y are the coordinates axis.

The jet initial velocity on weir crest is:

$$V_0 = \alpha V = \alpha\,(q/y_b) \tag{8}$$

being α the Coriolis coefficient and y_b the jet depth on weir crest.

The ratio between the pool depth under nappe, Y_u, and the water cushion, Y, is calculated with the Cui Guang Tao formulae (1985, revised by Castillo, 1989):

$$Y_u/Y = \sqrt{1 - 2F_D\left[\left(V_j/V_D\right)\beta cos\theta - 1\right]} \tag{9}$$

where $F_D = V_D^2/(gY)$ is the square Froude number, V_D is the downstream velocity in the water cushion, $\beta \approx 0.6$ is the head loss coefficient and θ is the impingement jet angle.

Turbulent Jets Device

The device of turbulent jets and energy dissipation in the nappe flow case (Figure 1), allows us to study air-water two-phase phenomena (aeration, spray, spread and impact). The mobile mechanism allows us to vary the discharge heights between 1.70 and 4.00 m and flows between 10 and 150 l/s. The plunge pool is a methacrylate´s box (1.60 m height and 1.05 m wide) in which can be regulated different water cushion. Instantaneous pressure measurements are registered with piezoresistive transducers located on plunge pool bottom, instantaneous velocities with ADV equipment and mean velocities and aeration rates with fiber optical instrumentation. In addition, the high-speed video instrumentation will permit us to characterize the turbulence phenomenon.

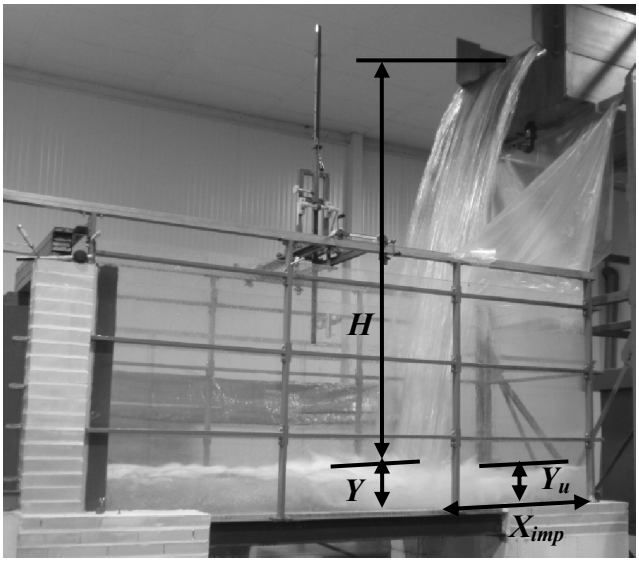

Figure 1: Structure of turbulent jets

Numerical Modeling

The main advantage of the methodology called "Computational Fluid Dynamics" (*CFD*) is the possibility it offers to investigate physical fluid systems, providing lot of data, increased profitability, flexibility and speed than that obtained with experimental procedures. However, to a correct use, it is necessary to contrast and to calibrate with data obtained in prototype or physics model.

In this paper, the *CFD* methodology is applied to the investigation of flows highly aerated and turbulent, using the programs *ANSYS CFX* (2009) and *FLOW 3D* (2011). The programs solve the differential equations of the phenomenon in control volumes defined by the meshing of the fluid domain, retaining the reference quantity (mass, momentum, energy) in the three directions for each control volume identified.

To complement the numerical solution of Reynolds equations and average Navier-Stokes (*RANS*), turbulence models has been used. There are many turbulent models of diverse complexity, from the isotropic models of two-equation like the classic k-ε to the second moment closure models (*SMC*) like the Reynolds Stress Model.

The *SMC* models are based on the solution of a transport equation for each of the independent Reynolds stresses in combination with the k-ε or the k-ω equation. The experience shows that the increased number of transport equations in the *SMC* models leads to reduced numerical robustness, requires increased computational effort and for this reason are rarely used.

The two equations models have been widely applied in the solution of many flows of engineering interest. The k-ε (*k-epsilon*) model, has been implemented in most general purpose *CFD* codes and is considered the industry standard model, but may not be suitable to solve flows with boundary layer separation. The k-ω based models try to give a highly accurate predictions of the flow separation.

In *ANSYS CFX* we used the k-ω based Shear-Stress-Transport (*SST*) model. This model was designed to give highly accurate predictions of the onset and the amount of flow separation under adverse pressure gradients by the inclusion of transport effects into the formulation of the eddy-viscosity. The best performance of this model has been demonstrated in a large number of validation studies (Bardina et al, 1997).

In *FLOW 3D* we used the k-ε model. Even though the based on Renormalization-Group (*RNG*) k-ε model is theoretically more accurate than the standard k-ε model, Wilcox (2006) obtained that the k-ε model seems to be more accurate than the *RNG* k-ε in plane jets.

In *ANSYS CFX* we have also used a Reynolds Stress model based on the ω-equation to solve the turbulent component velocities (u', v', w') in the falling jet.

To solve the two-phase air-water in *ANSYS CFX* we used the homogeneous model. It can be considered as a limit case of the inhomogeneous model, in which the transfer rate at the interface is very great. A common flow field is shared by all fluids, remained valid in flows domain by gravity when the phases are completely stratified (case of a free surface flow in which the interface is well defined).

In *FLOW 3D* we selected the one fluid option, joined the air entrainment, density evaluation and drift flux explicit models.

In the study of turbulent jets flow separation and high turbulence exist. They need high quality mesh elements in order to solve the problem with the highest accuracy. The mean difference among the different mesh elements is the number of nodes and their distribution. In this way, more node number drove to obtain better results.

We have used in both software hexahedral mesh elements. The total number of elements used in the *ANSYS CFX* simulation was 750,544 elements, with length scale in the falling jet boundary and at stagnation point of 0.01 m.

In *FLOW 3D* firstly we started modeling the failing jet boundary and the water cushion near the impact point with 0.005 m length scale, but it was observed that the mean pressure in the stagnation point was 1.62 meters, almost two times the lab measurements. Possibly due to the high horizontal velocity downstream the stagnation point (≈ 6 m/s), the flow sweeps the water cushion near the jet impact (see Figure 2). This seems to be related with the turbulence models available in *FLOW 3D*. However, if the mesh size is changed then you can correct this unreal situation. In this way, it was used 1,978,756 elements, with 0.005 m length scale in the falling jet boundary and 0.01 m in the water cushion.

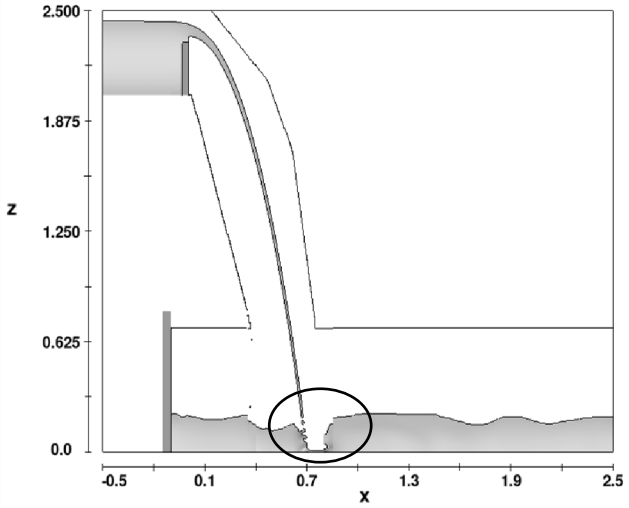

Figure 2: Sweep of the water cushion under the jet impact in *FLOW 3D*

The model boundary conditions correspond to the flow and turbulence inlet, upstream and downstream levels and their hydrostatic pressures distributions.

All scenarios have been calculated by a transient calculation time of 60 seconds and to obtain the results we have used a 20 Hz frequency, the same as used in the lab pressure measurements. In Figure 3 we can observe that permanent conditions are reached after 20 seconds of simulation. In *ANSYS CFX* we solved using a step interval of 0.05 seconds while in *FLOW 3D* we fixed the time step in 0.0001 seconds in order to avoid that the solver use a smaller time due to step stability solver criteria when the permanent condition starts.

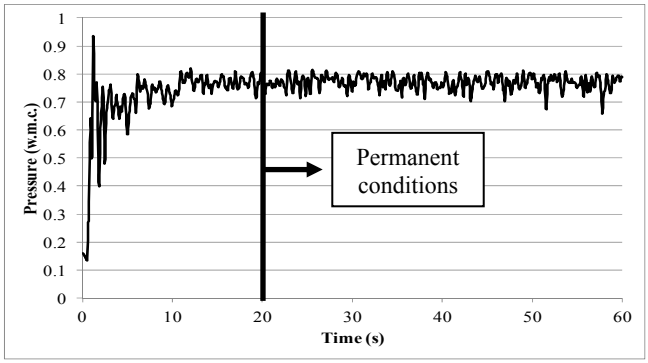

Figure 3: Transient of total pressure at the stagnation point of the plunge pool

The mean total wall clock time in *ANSYS CFX* was 4.099E+05 seconds (≈ 5 days) and 1.073E+06 seconds (≈ 12 days) in *FLOW 3D* in a CPU with 8 cores.

We have used the ratio 0.5 of Water Volume Fraction in order to obtain the free surface in the jet and in the stilling basin. Figure 4 shows the free surface obtained with the *CFD* programs when permanent conditions are reached. We can see that the jet profile is very similar to the lab jet shows in the description of the lab device.

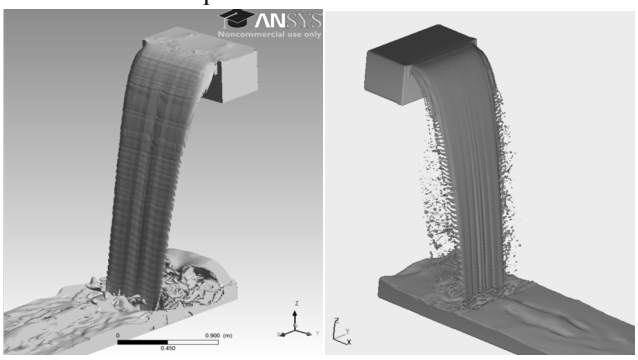

Figure 4: Free surface of turbulent jets solved with *ANSYS CFX* and *FLOW 3D* (q = 0.058m^2/s, H = 2.27m, h=0.087m, Y = 0.17m)

Results and Discussion

In order to entry the most accurate laboratory conditions in the numerical models, we measured the weir upstream section with Acoustic Doppler Velocimeter. In this way, we could know the real turbulence level in the inlet section. The measured section was located 0.50 m upstream the free discharge weir in order to avoid the perturbations near the weir.

The turbulent velocities measured with *ADV* methodology was used as input data in the numerical simulations.

In Figure 5 we can see the differences among the numerical solutions and the lab measurements in the pressure distribution at the stagnation point when permanent conditions are reached. *ANSYS CFX* obtains a little variability of pressure at the stagnation point while *FLOW 3D* shows a distribution more similar to the lab measurements.

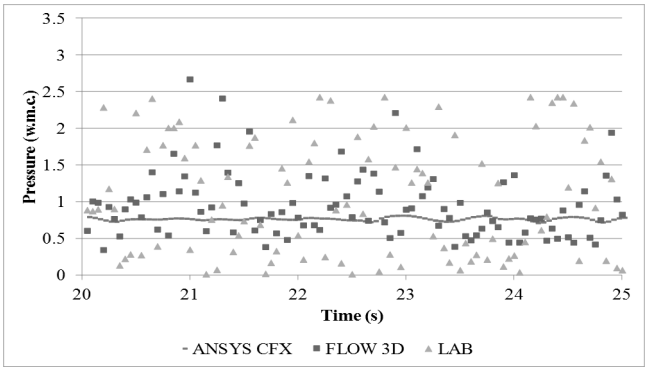

Figure 5: Pressure at the stagnation point of the plunge pool

Table 2 shows a comparison of the most important parameter that appears in the phenomenon of turbulent jets. Data were extracted from the numerical modeling carried out with *ANSYS CFX* and *FLOW 3D* and measurements in the Hydraulic Laboratory of the Universidad Politécnica de Cartagena. This data are compared too with the results proposed by Castillo (2006) and called here as Parametric methodology.

Table 2: Comparison of the principal measurement and calculated variables (q = 0.058m^2/s, H = 2.27m, h=0.087m, Y = 0.17m)

	CFX ($T_{u,x}$=0.16)	FLOW3D ($T_{u,x}$=0.16)	Lab	Param.
h (m)	0.089	0.087	0.087	0.087
y_b (m)	0.078	0.072	0.082	0.083
V_0 (m/s)	0.77	0.83	-	0.76
V_i (m/s)	1.78	1.87	-	1.54
B_i (m)	0.048	0.034	-	0.053
V_j (m/s)	6.32	6.76	-	6.59
B_j (m)	0.022	0.012	-	0.025
L_b (m)	> H	>H	-	3.12
X_{imp} (m)	0.75	0.70	0.74	0.73
H_m (w.c.m.)	0.92	0.86	0.85	1.10
Y_u (m)	0.12	0.18	0.16	0.17
Y (m)	0.16	0.17	0.17	0.17
θ (º)	82.75	82.18	-	81.58
C_p	0.37	0.30	0.34	0.41

In this table we can see that the four methodologies offer very similar results. In all of them we have effective cushion ($Y > 4\ B_j$). Also a solid core jet reaches the water cushion because there is not enough distance of fall to

produce the disintegration of the jet ($H<L_b$). The main differences correspond to the jet thickness obtained in *FLOW 3D* that are little smaller than the other methods. The calculation of Y_u in *ANSYS CFX* is difficult because of the high air entrainment rate in this point complicates the free surface visualization. On the other hand, the mean dynamic pressure coefficient obtained with Parametric methodology is bigger than the other due to the parameter of the Table 1 (obtained as upper envelope of lab measurements). This formulation is valid up to an inlet turbulence of 0.05.

Due to we have a high turbulence ($T_{u,x}$ =0.16) in the inlet of our physic dispositive, we considered necessary to know how different turbulence rates in the inlet affect the numerical solutions.

In order to know the turbulent parameter K_φ, we simulated the failing jets in *ANSYS CFX* using a second moment closure turbulent model based on the ω-equation. So, we have considered three different turbulences in the inlet condition ($T_{u,x}$=0.16, 0.03 and 0.01). Following a streamline we can see in the Figure 6 the evolution of T_u for each inlet turbulent intensity $T_{u,x}$.

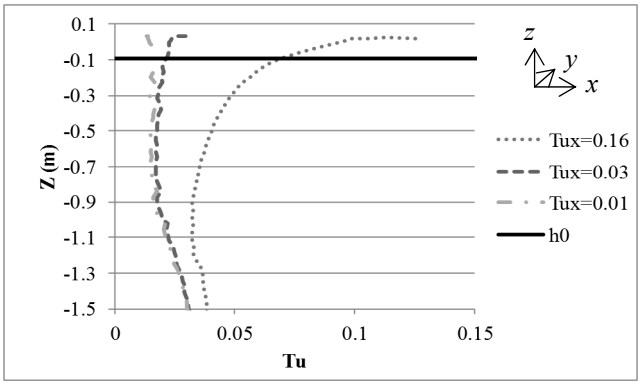

Figure 6: Evolution of the turbulence of the failing jet

This Figure shows us that, even thought the turbulences in the inlet condition are different, T_u tends to be equal when there are sufficient distance of fall from the weir.

In a similar way, we can see the evolution of the turbulent parameter K_φ (Figure 7).

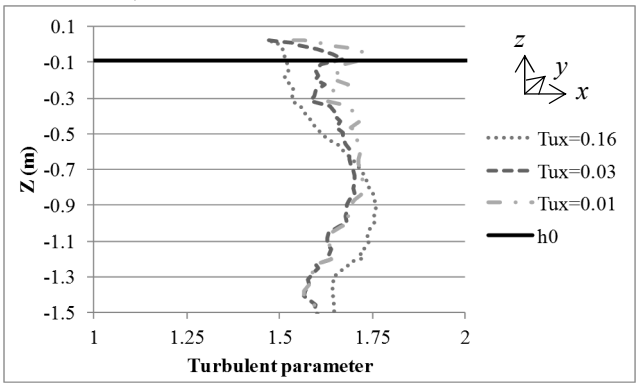

Figure 7: Evolution of the turbulent parameter K_φ

For this specific flow we observe in Figure 7 that K_φ is between 1.5 and 1.75.

Table 3 shows the results obtained in the initial conditions of the Parametric methodology (Z=-h), for different turbulences at the inlet condition.

Table 3: Turbulent velocities (u', v', w') in the initial conditions section (Z =-h), q=0.058m^2/s and h=0.087m

	CFX ($T_{u,x}$=*0.16*)	CFX ($T_{u,x}$=*0.03*)	CFX ($T_{u,x}$=*0.01*)
V_i (m/s)	1.78	1.67	1.65
u' (m/s)	5.765e-02	1.969e-02	1.543e-02
v' (m/s)	7.260e-02	2.096e-02	1.545e-02
w' (m/s)	8.484e-02	2.204e-02	1.546e-02
$\overline{V_t'}$ (m/s)	1.257e-01	3.623e-02	2.675e-02
T_u	7.060e-02	2.170e-02	1.621e-02
$\overline{V_t'} = f(w')$	1.48w'	1.64w'	1.73w'

In previous studies it was found that the turbulent parameter of plane jets is approximately 1.50 when $T_{u,x}$ in the inlet condition, is near to 16 %. The results of this study show that if the turbulence at the inlet condition decreases, the vertical turbulent velocity w' decreases, then the turbulent parameter increases to the value of $K_\varphi \approx 1.73$.

However, we need to follow working in order to get a universal relation between the inlet turbulent intensity and the turbulent parameter in the initial conditions.

Finally, Tables 4 and 5 shows the results obtained with *ANSYS CFX* and *FLOW 3D*, varying the turbulence in the inlet condition.

Table 4 shows that the variation of the turbulence at the inlet condition of *ANSYS CFX* only affects the mean pressure at the stagnation point and therefore vary the C_p while the other parameters have almost the same value.

Table 4: Comparison of the principal variables obtained with *ANSYS CFX* (q = 0.058m^2/s, H = 2.27m, h = 0.087m, Y = 0.17m)

	CFX ($T_{u,x}$=*0.16*)	CFX ($T_{u,x}$=*0.03*)	CFX ($T_{u,x}$=*0.01*)
h (m)	0.089	0.089	0.089
y_b (m)	0.078	0.077	0.078
V_0 (m/s)	0.77	0.79	0.79
V_i (m/s)	1.78	1.75	1.75
B_i (m)	0.048	0.048	0.047
V_j (m/s)	6.32	6.30	6.32
B_j (m)	0.022	0.023	0.022
L_b (m)	> H	> H	> H
X_{imp} (m)	0.75	0.75	0.74
H_m (w.c.m.)	0.92	0.84	0.86
Y_u (m)	0.12	0.10	0.115
Y (m)	0.16	0.16	0.16
θ (º)	82.75	82.42	82.49
C_p	0.37	0.34	0.34

Nevertheless, Table 5 shows that the variation of the turbulence not affects the results of *FLOW 3D*.

Table 5: Comparison of the principal variables obtained with *FLOW 3D* (q = 0.058 m^2/s, H = 2.27 m, h=0.087 m, Y = 0.17m)

	FLOW3D ($T_{u,x}$=*0.16*)	FLOW3D ($T_{u,x}$=*0.03*)	FLOW3D ($T_{u,x}$=*0.01*)
h (m)	0.087	0.087	0.087
y_b (m)	0.072	0.071	0.071
V_0 (m/s)	0.83	0.81	0.81
V_i (m/s)	1.87	1.84	1.84
B_i (m)	0.034	0.034	0.034
V_j (m/s)	6.76	6.80	6.74
B_j (m)	0.012	0.014	0.011
L_b (m)	>H	>H	>H
X_{imp} (m)	0.70	0.71	0.71
H_m (w.c.m.)	0.86	0.88	0.89
Y_u (m)	0.18	0.175	0.175
Y (m)	0.17	0.18	0.18
θ (º)	82.18	82.39	82.33
C_p	0.30	0.30	0.31

Conclusions

In order to improve the design of energy dissipation structures: arch dams, overtopping gravity dams, fall structures in channels, it is necessary to advance in the knowledge and characterization of the hydrodynamic actions.

The parametric methodology used in this paper is based only on the results of pressure measurements at the bottom of the stilling basin.

To advance knowledge in this area it is necessary to make more experimental studies, both physical models and prototypes, simultaneously characterizing the phenomena produced in the jets aeration and measures of pressures, velocities and aeration rates in stilling basins.

To conclude our comparison between *CFD* programs, we can say that *FLOW 3D* is not very accurate near stagnation points, forcing us to increase the mesh size, against the meshing theory. On the other hand, *ANSYS CFX* obtains a average pressures register in contrast to the natural variability of the phenomenon.

The laboratory results allow us to calibrate and validate some commercial programs *CFD*. As can see, progress in the characterization of the phenomenon of turbulent jets with *ANSYS CFX* and *FLOW 3D* are being made. Later we wish to validate the results with some Lagrangian program.

This is the objective of the present paper, whose results and conclusions will hopefully contribute to advance the understanding of these phenomena.

References

Annandale, G.W. (2006). Scour Technology. *McGraw-Hill*, N.Y, USA.

ANSYS CFX (2010). ANSYS CFX. *Reference Guide. Release 13.0*.

Armengou, J. (1991). Vertido libre por coronación presas bóveda. Análisis del campo de presiones en cuenco amortiguador. *PhD Thesis*. Universidad Politécnica de Cataluña, España.

Bardina, J.E., Huang, P.G. & Coakley, T.J. (1997). Turbulence Modeling Validation Testing and Development. *NASA Technical Mem.* 110446.

Bollaert, E. & Schleiss,A. (2003). Scour of rock due to the impact of plunging high velocity jets Part I: A state-ofthe-art review. *Journal of Hydraulic Research*, Vol. 41, No.5, pp. 451-464.

Castillo, L. (1989). Metodología experimental y numérica para la caracterización del campo de presiones en los disipadores de energía hidráulica. Aplicación al vertido libre en presas bóveda. *PhD Thesis.* Universidad Politécnica de Cataluña, España.

Castillo,L., Puertas,J. & Dolz,J. (1999). Discussion about pressure fluctuations on plunge pool floors. *Journal of Hydraulic Research,* Vol.37, No.2, pp. 272-788.

Castillo, L. (2002). Parametrical analysis of the ultimate scour and mean dynamic pressures at plunge pools. Proc. *École Polytechnique Fédérale de Lausanne*, Switzerland. Schleiss & Bollaert (eds). A.A. Balkema.

Castillo, L. (2006). Areated jets and pressure fluctuation in plunge pools. *The 7th International Conference on Hydroscience and Engineering* (ICHE-2006), IAHR, ASCE, Drexel University. College of Engineering. DSpace Digital Lybrary. DU Haggerty Library. Philadelphia, USA.

Castillo, L. (2007). Pressure characterization of undeveloped and developed jets in shallow and deep pool. *32nd Congress of IAHR, the International Association of Hydraulic Engineering & Research*, Vol.2, pp. 645-655, Venice, Italy.

Castillo, L., Puertas, J. & Dolz, J. (2007). Discussion about Scour of Rock due to the impact of plunging high velocity jets. *Journal of Hydraulic Research*, Vol. 45, No. 6, pp. 715-723.

Castillo, L. & Carrillo, J.M. (2011). Numerical simulation and validation of hydrodynamics actions in energy dissipation devices. *34th IAHR World Congress. International Association of Hydro-Environment Engineering and Research.* Brisbane, Australia.

Cui, G. T. (1985). Gongba yiliu shuishe dui hechuang zuoyonghi ji qi yinxiang de yanjui. *Shuli xuebao* (8), pp. 53-68. [Efeito do impacto, no leito do rio, da lamina descarregada sobre una barragem-abóbada. I.C.T. TR. 829 LNEC, Lisboa, 1986].

Davies, J.T. (1972). Turbulence phenomena. *Academic Press*, New York.

Ervine, D.A. & Falvey, H.R. (1987). Behaviour of turbulent jets in the atmosphere and plunge pools. *Proceedings of the Institutions of Civil Engineers*, Part. 2, Vol. 83, pp. 295-314.

Ervine, D.A., Falvey,H.T. & Withers,W.A. (1997). Pressure fluctuations on plunge pool floors. *Journal of Hydraulic Research*. Vol. 35, No. 2, pp. 257-279.

Federspiel, M.P. (2011). Response of an Embedded Block Impacted by High-Velocity Jets. *PhD Thesis.* École Politechnique Fédérale de Lausanne, Suisse.

FLOW 3D (2011). FLOW Sciense, Inc. *FLOW 3D. Theory v10.0.*

Manso, P.A., Bollaert, E.F.R. & Schleiss, A.J. (2005). Dynamic pressures generated by plunging jets in confined pools under extreme flood discharges. *XXXI IAHR Congress*, Seoul, CD_Rom, pp: 2848-2860.

Puertas, J. (1994). Criterios hidráulicos para el diseño de cuencos de disipación de energía en presas bóveda con vertido libre por coronación. *PhD Thesis*. Universidad Politécnica de Cataluña, España.

Scimeni, E. (1930). Sulla forma delle vene tracimanti. *L´Energia Elettrica*, Aprile, pp. 293-305.

Wilcox D.C. (2006). Turbulence modeling for CFD. *DCW Industries, Inc*.

Withers, W. (1991). Pressure fluctuation in plunge pool of an impinging jet spillway. *PhD Thesis*, University of Glasgow, United Kingdom.